

The influence of the broadness of the degree distribution on network's robustness: comparing localized attack and random attack

Xin Yuan,¹ Shuai Shao,¹ H. Eugene Stanley,¹ and Shlomo Havlin^{1,2}

¹*Center for Polymer Studies and Department of Physics, Boston University, Boston, MA 02215 USA*

²*Minerva Center and Department of Physics, Bar-Ilan University, Ramat-Gan 52900, Israel*

The stability of networks is greatly influenced by their degree distributions and in particular by their broadness. Networks with broader degree distributions are usually more robust to random failures but less robust to localized attacks. To better understand the effect of the broadness of the degree distribution we study here two models where the broadness is controlled and compare their robustness against localized attacks (LA) and random attacks (RA). We study analytically and by numerical simulations the cases where the degrees in the networks follow a Bi-Poisson distribution $P(k) = \alpha e^{-\lambda_1} \frac{\lambda_1^k}{k!} + (1 - \alpha) e^{-\lambda_2} \frac{\lambda_2^k}{k!}$, $\alpha \in [0, 1]$, and a Gaussian distribution $P(k) = A \cdot \exp\left(-\frac{(k-\mu)^2}{2\sigma^2}\right)$ with a normalization constant A where $k \geq 0$. In the Bi-Poisson distribution the broadness is controlled by the values of α , λ_1 and λ_2 , while in the Gaussian distribution it is controlled by the standard deviation, σ . We find that only for $\alpha = 0$ or $\alpha = 1$, namely degrees obeying a pure Poisson distribution, LA and RA are the same but for all other cases networks are more vulnerable under LA compared to RA. For Gaussian distribution, with an average degree μ fixed, we find that when σ^2 is smaller than μ the network is more vulnerable against random attack. However, when σ^2 is larger than μ the network becomes more vulnerable against localized attack. Similar qualitative results are also shown for interdependent networks.

I. INTRODUCTION

Complex networks are widely used as models to understand many features of complex systems, such as structure, stability and function [1–20]. Robustness of network suffering site or link attacks is of much interest, since it has been observed in many real-world networks. Approaches such as site percolation on a network where nodes suffer either random attack (RA) [2–4] or targeted attack (TA) based on nodes connectivity [2, 3] emerged to study these phenomena. A new type of attack, localized attack (LA), in which nodes surrounding a seed node are removed layer by layer, has been introduced recently [21, 22]. Moreover, interdependent networks have shown significantly more vulnerability under RA and TA compared to their single counterparts [23–29]. LA on spatially embedded interdependent networks has been addressed, and a significant metastable regime where LA above a critical size propagates throughout the whole system has been found [22].

Until now, well-defined tools have been established to probe the robustness of networks against all the aforementioned attack scenarios and the broadness of the degree distributions is found to be influential on the stability of networks [5]. However, a systematic study on the effect of the broadness of the degree distribution on robustness is still missing. Here we study and compare LA and RA on two networks models where the broadness is controlled. One model is a Bi-Poisson with two distinct groups having different average degrees. The difference between the two average degrees characterizes the broadness of the degree distribution of the network. Usually, research focused on a network with a pure Poisson degree distribution, but in many cases there could be two or more degree distributions in a network [30, 31]. For

example, a network of two groups of people, of whom one group has high degree (many friends) and the other has low degree (few friends), might be better captured as a Bi-Poisson distribution. Note that Bi-Poissonian networks were found to be optimally robust against TA [30]. The second model where the broadness can be controlled is a Gaussian degree distribution. Here, the standard deviation σ characterizes the broadness of the degree distribution. Such a distribution is realistic; e.g., the distribution of Web links has been found to resemble a Gaussian distribution [32].

Hence, we here analyze the robustness of networks with tunable broadness of degree distributions, such as Bi-Poisson and Gaussian degree distributions, under attack. Here, limiting ourselves to LA and RA only, we follow the frameworks developed in [4, 21] and extend them (i) to the study of single networks with a Bi-Poisson distribution and (ii) to the study of single networks with a Gaussian distribution and (iii) to the study of fully interdependent networks with the same Bi-Poisson distribution in each network and (iv) to the study of fully interdependent networks with the same Gaussian distribution in each network. By changing α of the Bi-Poisson distribution

$$P(k) = \alpha e^{-\lambda_1} \frac{\lambda_1^k}{k!} + (1 - \alpha) e^{-\lambda_2} \frac{\lambda_2^k}{k!}, \alpha \in [0, 1] \quad (1)$$

with fixed λ_1 and λ_2 , and σ^2 of the Gaussian distribution

$$P(k) = A \cdot \exp\left(-\frac{(k-\mu)^2}{2\sigma^2}\right), k \geq 0 \quad (2)$$

with μ fixed, we investigate how the distribution broadness influences the percolation properties. These include the critical threshold p_c at which the giant component P_∞ first collapses, and the size of the giant components

P_∞ as a function p , the fraction of unremoved nodes. In all cases, extensive simulations and analytical calculations are performed, showing good agreement with each other. Qualitative characteristics about robustness of both single and interdependent networks under LA and RA are presented.

II. RA AND LA ON A SINGLE NETWORK

A. Theory

As in Ref. [33], we introduce the generating function of the degree distribution $P(k)$ of a certain network as

$$G_0(x) = \sum_k P(k)x^k. \quad (3)$$

Similarly, for the generating function of the underlying branching processes, we have

$$G_1(x) = \sum_k \frac{P(k)k}{\langle k \rangle} x^{k-1} = \frac{G'_0(x)}{G'_0(1)}. \quad (4)$$

Likely, the size distribution of the clusters that can be reached from a randomly chosen link is generated in a self-consistent equation

$$H_1(x) = xG_1(H_1(x)). \quad (5)$$

Then the size distribution of the clusters that can be traversed by randomly following a starting vertex is generated by

$$H_0(x) = xG_0(H_1(x)). \quad (6)$$

Next we distinguish between random attack and localized attack.

(I) *Random Attack*: An initial attack with the random removal of a fraction $1 - p$ of nodes from the network will result in changing the cluster size distribution of the remaining network, so that the generating functions of the surviving clusters' size distribution are [4]

$$H_1(x) = 1 - p + pxG_1(H_1(x)), \quad (7)$$

and analogously,

$$H_0(x) = 1 - p + pxG_0(H_1(x)). \quad (8)$$

Now p_c , the critical value at which the giant component collapses, is determined by the following equation

$$p_c = \frac{1}{G'_1(1)}, \quad (9)$$

namely,

$$p_c = \frac{1}{G'_1(1)} = \frac{G'_0(1)}{G''_0(1)}, \quad (10)$$

which is equivalent to the expression $p_c = \langle k \rangle / \langle k(k-1) \rangle$ found in [3].

Thus, for a Bi-Poisson distribution, since we have $G_0(x) = \alpha e^{\lambda_1(x-1)} + (1-\alpha) e^{\lambda_2(x-1)}$, p_c can be obtained as

$$p_c = \frac{\alpha \lambda_1 + (1-\alpha) \lambda_2}{\alpha \lambda_1^2 + (1-\alpha) \lambda_2^2}. \quad (11)$$

For a Gaussian distribution we have

$$p_c = \frac{\sum_1^\infty k e^{-(k-\mu)^2/2\sigma^2}}{\sum_2^\infty k(k-1) e^{-(k-\mu)^2/2\sigma^2}}. \quad (12)$$

And the size of the resultant giant component is [4]

$$P_\infty(p) = 1 - H_0(1) = p[1 - G_0(H_1(1))], \quad (13)$$

which can be numerically determined by solving $H_1(1)$ from its self-consistent equation

$$H_1(1) = 1 - p + pG_1(H_1(1)). \quad (14)$$

(II) *Localized Attack*: We next consider the initial removal of a fraction $1 - p$ of nodes locally, starting with a randomly chosen seed node. In this case one removes this seed node and its nearest neighbors, next nearest neighbors etc. until a fraction $1 - p$ of nodes are removed from the network. This kind of attack may be realistic in cases such as earthquakes or in cases of weapons of mass destruction. As in [21], the localized attack can be separated into two stages: (i) at the first stage nodes belonging to the attacked area (the seed node and the layers surrounding it) are removed but the links connecting them to the remaining nodes of the network are kept; (ii) at the second stage, these links are also removed. Following the method introduced in [21, 34], we get the generating function of the degree distribution of the remaining network as

$$G_{p0}(x) = \frac{1}{G_0(f)} G_0[f + \frac{G'_0(f)}{G'_0(1)}(x-1)], \quad (15)$$

where $f \equiv G_0^{-1}(p)$. Therefore, the generating function of the underlying branching processes is

$$G_{p1}(x) = \frac{G'_{p0}(x)}{G'_{p0}(1)}. \quad (16)$$

The generating function of the cluster size distribution following a random starting node in the remaining network is

$$H_{p0}(x) = xG_{p0}(H_{p1}(x)), \quad (17)$$

where $H_{p1}(x)$, standing for the generating function of the cluster size distribution by randomly traversing a link, satisfies the self-consistent condition

$$H_{p1}(x) = xG_{p1}(H_{p1}(x)). \quad (18)$$

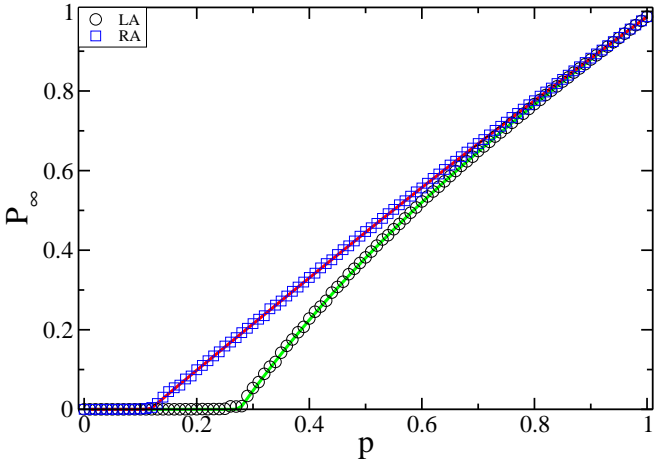


FIG. 1. (Color online) Sizes of giant component, $P_\infty(p)$, as a function of p for $\lambda_1 = 4$, $\lambda_2 = 12$ and $\alpha = 0.7$. Here solid lines are theoretical predictions, from Eq. (13) for RA (red line) and Eq. (20) for LA (green line), and symbols are simulation results with network size $N = 10^4$, where averages are taken over 10 realizations, under LA (\bigcirc) and RA (\square).

The condition for the network to start having a giant component is $G'_{p1}(1) = 1$ [21], which yields p_c as the solution of

$$G''_0(G_0^{-1}(p_c)) = G'_0(1). \quad (19)$$

The size of the giant component $P_\infty(p)$ as a fraction of the remaining network thus satisfies [21],

$$P_\infty(p) = p [1 - G_{p0}(H_{p1}(1))], \quad (20)$$

which can be numerically determined by first solving $H_{p1}(1)$ from Eq. (18), i.e. $H_{p1}(1) = G_{p1}(H_{p1}(1))$.

In order to get p_c explicitly, we first need to get f_c from equation $f_c \equiv G_0^{-1}(p_c)$, namely f_c from $G_0(f_c) = p_c$. And then from Eq. (19), f_c must also satisfy $G''_0(f_c) = G'_0(1)$. In the general case, p_c and P_∞ can be obtained only by solving numerically Eqs. (19) and (20). In certain limiting cases, however, one can derive explicit analytical expressions for p_c from which more physical insight can be obtained. An example of such a specific case is given in the next subsection.

1. Analytic solution of p_c for Bi-Poisson distribution with $\lambda_2 = 2\lambda_1$

For a Bi-Poisson distribution, using its generating function and $G_0(f_c) = p_c$, f_c and p_c satisfy the relation

$$G_0(f_c) = \alpha[e^{(f_c-1)}]^{\lambda_1} + (1-\alpha)[e^{(f_c-1)}]^{\lambda_2} = p_c. \quad (21)$$

Assuming $\lambda_2 = 2\lambda_1$, we denote $e^{\lambda_1(f_c-1)} = y$ such that Eq. (21) reduces to $\alpha y + (1-\alpha)y^2 = p_c$, which, for $\alpha \neq 1$, is a quadratic equation of y and its positive solution is

$$y = \frac{\sqrt{\alpha^2 + 4p_c(1-\alpha)} - \alpha}{2(1-\alpha)}. \quad (22)$$

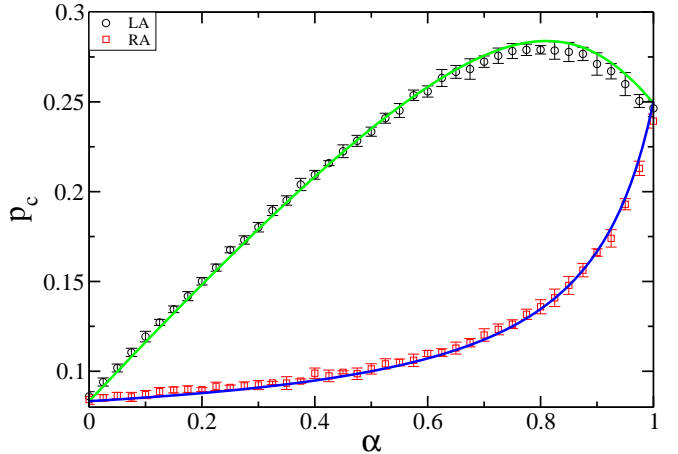


FIG. 2. (Color online) Percolation thresholds p_c of a single Bi-Poisson network as a function of α under LA and RA with $\lambda_1 = 4$, $\lambda_2 = 12$. Here solid lines are theoretical predictions, from Eq. (11) for RA (blue line) and Eq. (19) for LA (green line) and symbols (\square for RA and \bigcirc for LA) with error bars are simulation results with network size of $N = 10^4$ nodes, where averages and standard deviations are taken over 20 realizations.

Plugging f_c into Eq. (19) we get another quadratic equation of y

$$\alpha\lambda_1^2y + (1-\alpha)\lambda_2^2y^2 = \alpha\lambda_1 + (1-\alpha)\lambda_2, \quad (23)$$

for which the physical solution of y is

$$y = \frac{\sqrt{\alpha^2\lambda_1^4 + 4(1-\alpha)\lambda_2^2[\alpha(\lambda_1 - \lambda_2) + \lambda_2]} - \alpha\lambda_1^2}{2(1-\alpha)\lambda_2^2}. \quad (24)$$

Since $f_c = \ln(y)/\lambda_1 + 1$ and to obtain p_c we need to equate Eqs. (22) and (24); thus, we obtain

$$p_c = \frac{1}{64(1-\alpha)}[\beta + 6\alpha\sqrt{\alpha^2 + \beta} - 6\alpha^2], \quad (25)$$

where $\beta = \frac{16(1-\alpha)(2-\alpha)}{\lambda_1}$ and the relation of $\lambda_2 = 2\lambda_1$ has been used for simplification. Plugging $\alpha = 0$ into Eq. (25), we get $p_c = 1/\lambda_2$ as found in [21]. Also, for $\alpha \rightarrow 1$, employing L'Hôpital's rule we get $\lim_{\alpha \rightarrow 1} p_c = 1/\lambda_1$, as found in a pure Poisson distribution above.

Deriving p_c explicitly for a Gaussian distribution is not possible. Even for a Bi-Poisson distribution, other than special cases like the one discussed above, deriving p_c is also not possible as it requires solving first $f_c = G_0^{-1}(p_c)$, namely f_c from Eq. (21), which could be viewed as $\alpha y^{\lambda_1} + (1-\alpha)y^{\lambda_2} = p_c$, a polynomial equation of $y = e^{(f_c-1)}$. Since in this paper, we consider also the cases of $\lambda_2 > \lambda_1 \geq 4$ and according to Abel-Ruffini theorem, there is no general algebraic solution to the above equation except some special cases. Hence Newton's Method is employed to solve p_c and P_∞ numerically.

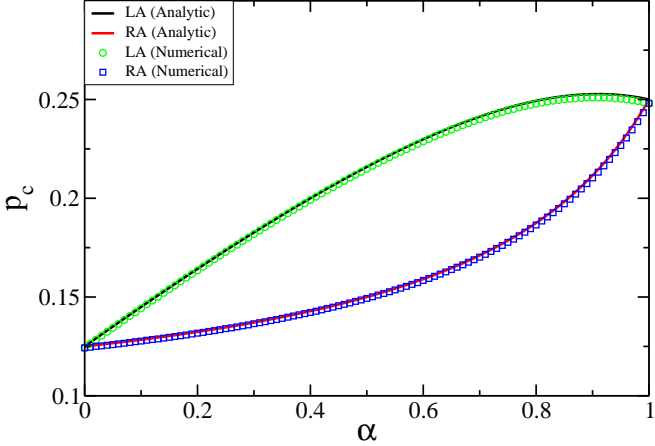


FIG. 3. (Color online) Comparison between numerical results (symbols) and the analytic results (solid lines) for Bi-Poisson distribution with $\lambda_1 = 4$ and $\lambda_2 = 8$. Note that they agree with each other well. Here, all the analytic results are obtained from Eq. (11) for RA (red line) and Eq. (25) for LA (black line) and the numerical results are attained by employing Newton's Method on Eqs. (11) and (19) respectively.

B. Results

To test the analytical predictions above we conducted numerical calculations of analytic expressions, and compared these results with simulation results on single networks with degrees following Bi-Poisson distributions as well as Gaussian distributions under both LA and RA. All the simulation results are obtained for networks of $N = 10^4$ nodes.

1. Single Bi-Poisson networks

Fig. 1 shows the giant component $P_\infty(p)$ as a function of the occupation probability p under LA and RA. Note that p_c is larger for LA compared to RA. The simulation results agree well with theoretical results obtained from Eqs. (13) and (20) and a second-order percolation transition behavior is present in both attack scenarios. Notice that when $\alpha = 0$ or 1 , i.e., degrees of nodes follow a pure Poisson distribution, as reported in [21], and the networks have the same critical value of p_c under LA and RA and the same dependence of $P_\infty(p)$ on p ; however here with $\alpha = 0.7$, we have $p_c(LA) > p_c(RA)$ indicating that the network is more fragile under LA compared to RA and the giant components behave differently.

The influence of the broadness of the distribution, tuned by changing α with fixed λ_1 and λ_2 , on the robustness of the network under LA and RA is shown in Fig. 2 where solid lines are numerical results from Newton's Method and symbols with error bars are simulation results. Notice that only for $\alpha = 0$ and $\alpha = 1$, we have $p_c(LA) = p_c(RA)$, otherwise $p_c(LA) > p_c(RA)$, showing that the network is always more vulnerable under LA

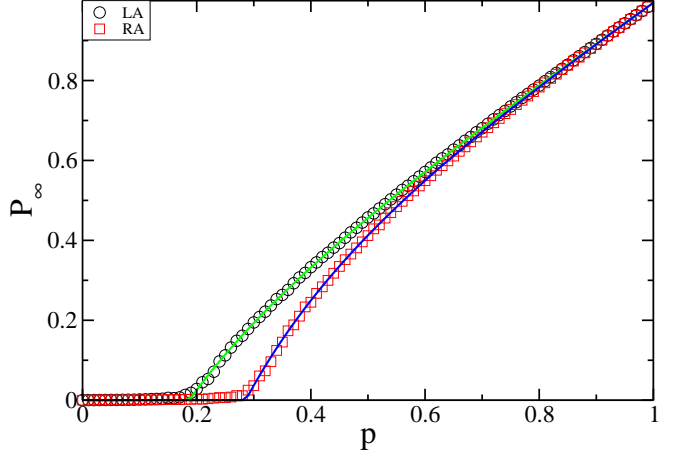


FIG. 4. (Color online) Sizes of giant component as a function of p of a single Gaussian network with $\mu = 4$ and $\sigma^2 = 2$. Here solid lines are theoretical results, from Eq. (13) for RA (blue line) and Eq. (20) for LA (green line) and symbols are simulation results obtained from network size of $N = 10^4$ where averages are taken over 10 realizations under LA (○) and RA (□).

than under RA if degrees follow a Bi-Poisson distribution. Notice also that $p_c(LA)$ peaks at $\alpha = 0.79$.

For the special case of $\lambda_2 = 2\lambda_1$, we compare the analytical values of p_c from Eqs. (11) and (25) using $\lambda_1 = 4$ and $\lambda_2 = 8$ with results obtained from Newton's Method (see Fig. 3). For this combination of average degrees, $p_c(LA)$ peaks at $\alpha = 0.91$. Notice that they agree well with each other showing that Newton's Method can deliver satisfactory results and therefore in the general case where $\lambda_2 \neq 2\lambda_1$ and in the cases of Gaussian distribution, it is used to get $p_c(LA)$.

2. Single Gaussian Networks

Fig. 4 shows the giant component $P_\infty(p)$ as a function of the occupation probability p under LA and RA respectively for a single network with Gaussian degree distribution. Note that simulation results agree well with theoretical results obtained from Eqs. (13) and (20) and a second-order phase transition behavior is present for both attack scenarios. Notice here that $\mu = 4$ and $\sigma^2 = 2$, and we have $p_c(LA) < p_c(RA)$ which indicates that the network is more robust under LA than RA for this particular distribution.

Further, with μ fixed, we find that when the Gaussian distribution gets broader, i.e., σ increases, $p_c(RA)$ decreases whereas $p_c(LA)$ increases with σ (see Fig. 5). Notice that, if $\sigma^2 < \mu$, then $p_c(LA) < p_c(RA)$; while the opposite when $\sigma^2 > \mu$. We also see that if $\sigma^2 \approx \mu$, then we have a crossing point with $p_c(RA) \approx p_c(LA)$, which is analogous to a Poisson ER networks with the same mean and variance, thus rendering the same robustness of the network under both LA and RA as reported in [21].

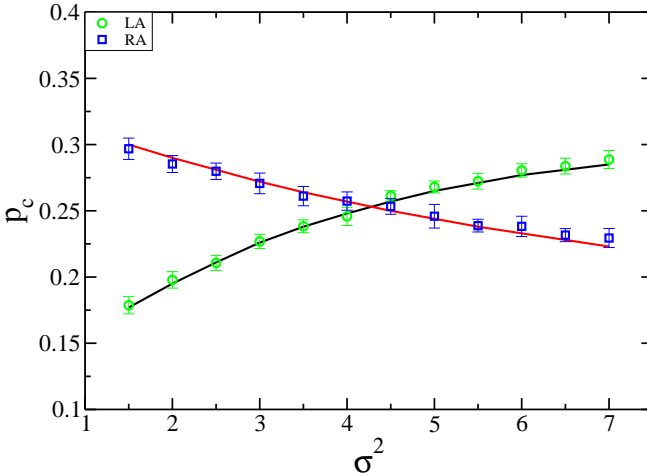


FIG. 5. (Color online) Percolation thresholds p_c as a function of σ^2 of networks with Gaussian degree distribution under LA and RA with $\mu = 4$. Here solid lines are theoretical predictions, from Eq. (12) for RA (red line) and Eq. (19) for LA (black line) and symbols (\square for RA and \circ for LA) with error bars are simulation results with network size of $N = 10^4$ nodes, where averages and standard deviations are taken over 20 realizations. It is shown here that as σ^2 increases $p_c(LA)$ increases whereas $p_c(RA)$ decreases simultaneously and they intersect each other around $\sigma^2 \approx \mu = 4$.

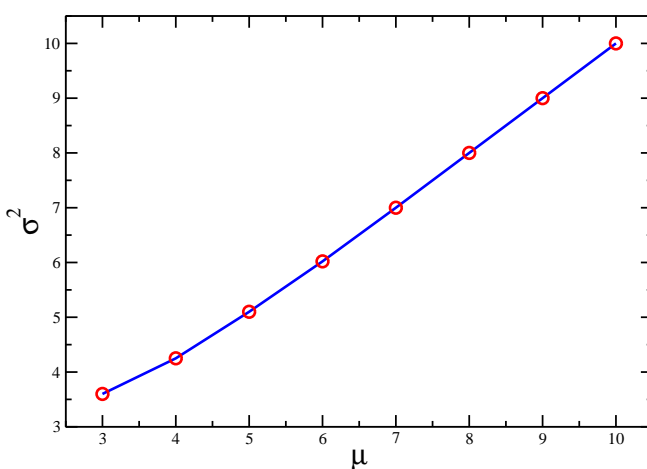


FIG. 6. (Color online) σ^2 as a function of μ at the intersection point where $p_c(LA) = p_c(RA)$ for single networks where degrees follow a Gaussian distribution.

Indeed in Fig. 6, we plot σ^2 as a function of μ when this particular intersection point occurs, namely $p_c(LA) = p_c(RA)$. Notice that except for some minor deviations at small μ values because the Gaussian distribution is deformed as we require $k \geq 0$, and the region above the extrapolation curve corresponds to $p_c(LA) > p_c(RA)$ whereas the region below this curve corresponds to $p_c(LA) < p_c(RA)$.

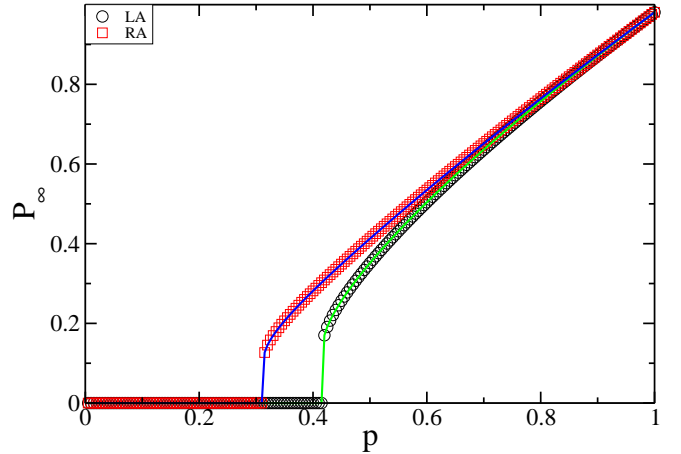


FIG. 7. (Color online) Sizes of the mutually connected giant component of the fully interdependent Bi-Poisson networks as a function of p for $\lambda_1 = 4$, $\lambda_2 = 12$ and $\alpha = 0.5$. Here solid lines are theoretical predictions, from Eq. (26) for RA (blue line) and similarly for LA (green line), and symbols are simulation results with network size $N = 10^4$, where averages are taken over 10 realizations, under LA (\circ) and RA (\square).

III. RA AND LA ON FULLY INTERDEPENDENT NETWORKS

A. Theory

We apply the formalism of RA on fully interdependent networks introduced in [23]. Specifically, we consider two networks A and B with the same number of nodes N . Within each network, the nodes are randomly connected with degree distribution $P_A(k)$ and $P_B(k)$ respectively. Each and every node in network A depends on a random node in network B , and vice versa. Also, we assume that if a node i in network A depends on the node j in network B and node j depends on the node l in network A , then $l = i$, which rules out the feedback condition [35]. This full interdependency means that every node i in network A has a dependent node j in network B , and if node i fails, so will node j , and vice versa.

(I) *Random Attack*: We begin by randomly removing a fraction $1 - p$ of nodes and their links within network A and all the nodes in network B that are dependent on the removed nodes in network A are also removed along with their connectivity links. As nodes and links are sequentially removed, each network begins breaking down into connected components. Due to interdependency, the removal process iterates back and forth between these two networks until they completely fragment or reach a mutually connected giant component with no further disintegration. As in Ref. [23] we introduce the function $g_A(p) = 1 - G_{A0}[1 - p(1 - f_A)]$ which is the fraction of nodes that belong to the giant component of network A , where f_A is a function of p that satisfies the transcendental equation $f_A = G_{A1}[1 - p(1 - f_A)]$. Similar equations exist for network B . After the system of the interdepen-

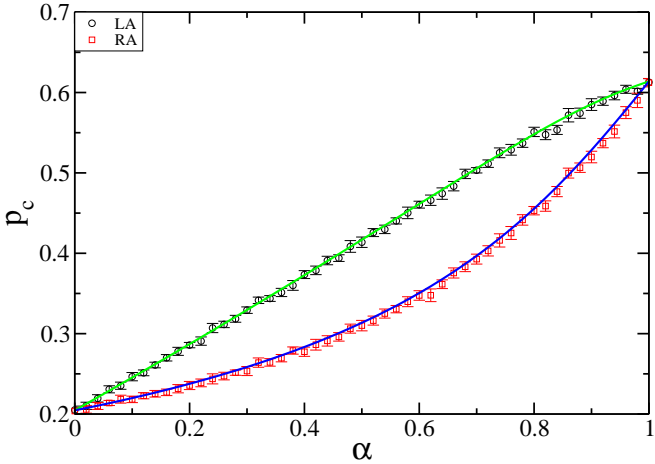


FIG. 8. (Color online) Percolation thresholds p_c of the fully interdependent Bi-Poisson networks with $\lambda_1 = 4$, $\lambda_2 = 12$ as a function of α under LA and RA. Here solid lines are theoretical predictions, from Eq. (29) for RA (blue line) and similarly for LA (green line) and symbols (\square for RA and \bigcirc for LA) with error bars are simulation results with network size of $N = 10^4$ nodes, where averages and standard deviations are taken from 20 realizations. When α is not 1 or 0, $p_c(LA)$ is always larger than $p_c(RA)$.

dent networks stops disintegrating, the fraction of nodes in the mutual giant component is P_∞ , satisfying

$$P_\infty = xg_B(x) = yg_A(y), \quad (26)$$

where x and y satisfy

$$x = pg_A(y), y = pg_B(x). \quad (27)$$

Excluding the trivial solution $x = 0, y = 0$ of the equation set above, we can combine them into a single equation by substitution and obtain,

$$x = g_A[g_B(x)p]p. \quad (28)$$

A nontrivial solution emerges in the critical case ($x = x_c, p = p_c$) by equating the derivatives of both sides of Eq. (28) with respect to x

$$1 = p^2 \frac{dg_A[pg_B(x)]}{dx} \frac{dg_B(x)}{dx} \Big|_{x=x_c, p=p_c} \quad (29)$$

which, together with Eq. (27), gives the solution for p_c and the critical size of the mutually connected component, $P_\infty(p_c) = x_c g_B(x_c)$.

(II) *Localized Attack*: When LA is performed on the one-to-one fully interdependent networks A and B described above, we can simply find an equivalent random network E with generating function $G_{E0}(x)$ such that after a random attack by removing $1 - p$ fraction of nodes in network E , the generating function of the remaining network is the same as $G_{p0}(x)$ (with the substitution of $G_0(x)$ by $G_{A0}(x)$). Then the LA problem on networks A and B can be mapped to a RA problem on networks

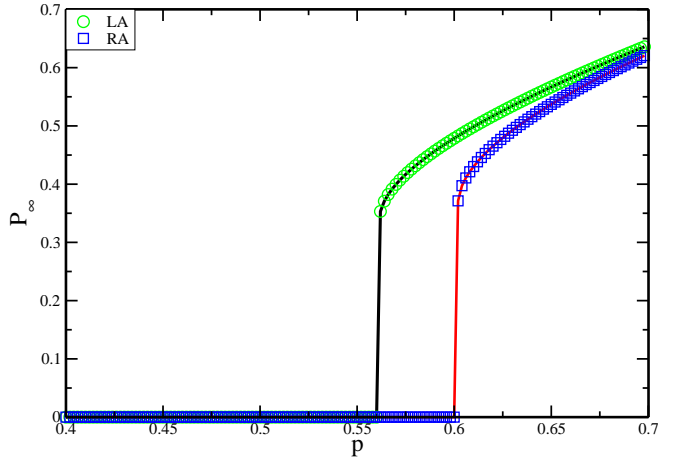


FIG. 9. (Color online) Sizes of mutual giant component of the fully interdependent Gaussian networks as a function of p with $\mu = 4$ and $\sigma^2 = 2$. Here solid lines are theoretical predictions, from Eq. (26) for RA (red line) and similarly for LA (black line), and symbols are simulation results with network size $N = 10^4$, where averages are taken over 10 realizations, under LA (\bigcirc) and RA (\square).

E and B . By using $G_{E0}(1 - p + px) = G_{p0}(x)$ and from Eq. (15) we have

$$G_{E0}(x) = \frac{1}{G_{A0}(f)} G_{A0}[f + \frac{G'_{A0}(f)}{G'_{A0}(1)G_{A0}(f)}(x - 1)]. \quad (30)$$

Thus, by mapping the LA problem on interdependent networks A and B to a RA problem on a transformed pair of interdependent networks E and B , we can apply the mechanism of RA on interdependent networks to solve p_c and $P_\infty(p)$ under LA.

It's easy to see that for pure Poisson distributions, $f \equiv G_{A0}^{-1}(p) = \frac{\ln(p)}{\lambda} + 1$ and by substituting f into Eq. (30) we will end up with $G_{E0}(x) = G_{A0}(x)$. Thus, for pure Poisson distributions, we will have exactly the same percolation properties for fully interdependent networks under LA with that under RA, as found in [23]. However, due to the complexities of the equations above, it is very difficult to obtain explicit expressions for p_c and $P_\infty(p)$ except for quite simple degree distributions, and thus we resort to numerical calculations in general.

B. Results

1. Fully interdependent networks with Bi-Poisson degree distribution

For two fully interdependent networks where the degrees in each network follow the same Bi-Poisson distribution, we carry out RA on one of the networks to initiate the cascading failure process until equilibrium. With the same set-up, we also carry out LA on one of the networks to launch the cascading failure process until equilibrium

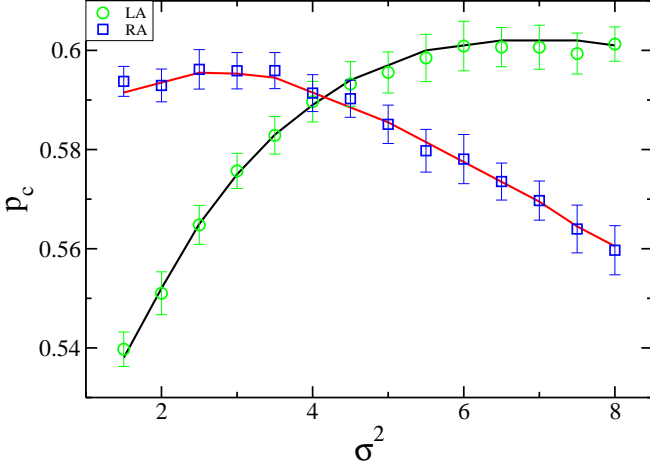


FIG. 10. (Color online) Percolation thresholds p_c as a function of σ^2 of the fully interdependent Gaussian networks under LA and RA with $\mu = 4$. Here solid lines are theoretical predictions, from Eq. (29) for RA (red line) and similarly for LA (black line) and symbols (\square for RA and \bigcirc for LA) with error bars are simulation results with network size of $N = 10^4$ nodes, where averages and standard deviations are taken from 20 realizations. It is seen here that as σ^2 increases $p_c(LA)$ increases and $p_c(RA)$ has a tendency to decrease. As σ^2 approaches the value of μ , $p_c(LA) \approx p_c(RA)$, which is manifested by the intersection point shown here.

is reached. Fig. 7 shows the sizes of the giant component $P_\infty(p)$ of the system as a function of the occupation probability p under LA and RA. Note that simulation results agree well with theoretical results obtained from Eq. (26) for both RA and LA scenarios, indicating that our strategy of finding an equivalent network under LA works well. Demonstrating a first-order phase transition behavior for both attack scenarios, the system is much more vulnerable compared to single networks under attack due to interdependency. Here with $\alpha = 0.5$, the system presents more fragility under LA compared to RA with $p_c(LA) > p_c(RA)$ and the giant components behave differently.

The influence of the broadness of the distribution, tuned by changing α with fixed λ_1 and λ_2 , on the robustness of the network under LA and RA is shown in Fig. 8 where solid lines are numerical results from applying Newton's Method on Eq. (29) and symbols with error bars are simulation results. Notice that only for $\alpha = 0$ and $\alpha = 1$, $P(k)$ is reduced to a pure Poisson and we have $p_c(LA) = p_c(RA) = 2.4554/\langle k \rangle$, as in [23]. However, if α deviates from 0 or 1, i.e., $P(k)$ deviates from a pure Poisson distribution and takes the form of a Bi-Poisson distribution, we will always have $p_c(LA) > p_c(RA)$, indicating the system is more vulnerable under LA than under RA.

2. Fully interdependent networks with Gaussian degree distribution

For two fully interdependent networks where the degrees in each network follow the same Gaussian distribu-

tion, we carry out RA on one of the networks to initiate the cascading failure process until reaching a steady state. With the same set-up, we also carry out LA on one of the networks to launch the cascading failure process until equilibrium is reached. Fig. 9 shows the sizes of the giant component $P_\infty(p)$ as a function of the occupation probability p under LA and RA. Note that simulation results agree well with theoretical results obtained from Eq. (26). The results demonstrate a first-order phase transition behavior for both attack scenarios; however, the system is much more vulnerable compared to single networks under attack due to interdependency. Here with $\mu = 4$ and $\sigma^2 = 2$, the system represents more fragility under LA compared to RA with $p_c(LA) < p_c(RA)$ and the giant components behave differently.

Further, with μ fixed, we find that when the Gaussian distribution gets broader, i.e., as σ increases, analogous to what we find in a single Gaussian network, the system shows different behaviors of the critical p_c against LA and RA. More specifically, Fig. 10 shows the effect of σ on p_c of the fully interdependent Gaussian networks where if $\sigma^2 < \mu$, then $p_c(LA) < p_c(RA)$; the opposite occurs if $\sigma^2 > \mu$. Again, the intersection point in this figure happens near the point $\sigma^2 \approx \mu$ similar to the Poisson distribution networks and thus the system behaves the same under LA as that under RA, as found in the previous subsection.

IV. CONCLUSIONS

In summary, we show that LA on interdependent networks can be mapped to a RA problem by transforming the network under initial attack. We also show how the broadness of the degree distribution affects the robustness of networks against RA and LA respectively. We show here that generally the broader the degree distribution is the more risky the networks are under LA compared to RA, which holds for both single networks as well as interdependent networks.

ACKNOWLEDGMENTS

We wish to thank ONR, DTRA, NSF, the European MULTIPLEX, CONGAS and LINC projects, DFG, the Next Generation Infrastructure (Bsim) and the Israel Science Foundation for financial support. We also thank the FOC program of the European Union for support.

[1] D. J. Watts and S. H. Strogatz, *Nature* **393**, 440 (1998).

[2] R. Albert, H. Jeong, and A.-L. Barabási, *Nature* **406**, 378 (2000).

[3] R. Cohen, K. Erez, D. Ben-Avraham, and S. Havlin, *Phys. Rev. Lett.* **85**, 4626 (2000).

[4] D. S. Callaway, M. E. Newman, S. H. Strogatz, and D. J. Watts, *Phys. Rev. Lett.* **85**, 5468 (2000).

[5] R. Albert and A.-L. Barabási, *Rev. Mod. Phys.* **74**, 47 (2002).

[6] M. E. Newman, *SIAM Rev.* **45**, 167 (2003).

[7] C. Song, S. Havlin, and H. A. Makse, *Nature* **433**, 392 (2005).

[8] G. Caldarelli and A. Vespignani, *Large scale structure and dynamics of complex networks: from information technology to finance and natural science*, vol. 2 (World Scientific, 2007).

[9] V. Rosato et al., *Int. J. Crit. Infrastruct.* **4**, 63 (2008).

[10] A. Arenas, A. Díaz-Guilera, J. Kurths, Y. Moreno, and C. Zhou, *Physics Reports* **469**, 93 (2008).

[11] R. Cohen and S. Havlin, *Complex networks: structure, robustness and function* (Cambridge University Press, 2010).

[12] M. Newman, *Networks: An Introduction* (Oxford University Press, 2010).

[13] G. Li et al., *Phys. Rev. Lett.* **104**, 018701 (2010).

[14] C. M. Schneider et al., *Proc. Natl. Acad. Sci.* **108**, 3838 (2011).

[15] A. Bashan et al., *Nature Commun.* **3**, 702 (2012).

[16] S. N. Dorogovtsev and J. F. Mendes, *Evolution of networks: From biological nets to the Internet and WWW* (Oxford University Press, 2013).

[17] J. Ludescher et al., *Proc. Natl. Acad. Sci.* **110**, 11742 (2013).

[18] X. Yan, Y. Fan, Z. Di, S. Havlin, and J. Wu, *PloS one* **8**, e69745 (2013).

[19] S. Boccaletti et al., *Physics Reports* **544**, 1 (2014).

[20] D. Li et al., *Proc. Natl. Acad. Sci.* **112**, 669 (2015).

[21] S. Shao, X. Huang, H. E. Stanley, and S. Havlin, *New J. Phys.* **17**, 023049 (2015).

[22] Y. Berezin, A. Bashan, M. M. Danziger, D. Li, and S. Havlin, *Scientific Reports* **5**, 8934 (2015).

[23] S. V. Buldyrev, R. Parshani, G. Paul, H. E. Stanley, and S. Havlin, *Nature* **464**, 1025 (2010).

[24] X. Huang et al., *Phys. Rev. E* **83**, 065101 (2011).

[25] T. P. Peixoto and S. Bornholdt, *Phys. Rev. Lett.* **109**, 118703 (2012).

[26] G. Baxter, S. Dorogovtsev, A. Goltsev, and J. Mendes, *Phys. Rev. Lett.* **109**, 248701 (2012).

[27] G. Dong, J. Gao, L. Tian, R. Du, and Y. He, *Phys. Rev. E* **85**, 016112 (2012).

[28] A. Bashan, Y. Berezin, S. V. Buldyrev, and S. Havlin, *Nature Physics* **9**, 667 (2013).

[29] F. Radicchi and A. Arenas, *Nature Physics* **9**, 717 (2013).

[30] A. X. Valente, A. Sarkar, and H. A. Stone, *Phys. Rev. Lett.* **92**, 118702 (2004).

[31] T. Tanizawa, G. Paul, S. Havlin, and H. E. Stanley, *Phys. Rev. E* **74**, 016125 (2006).

[32] D. M. Pennock, G. W. Flake, S. Lawrence, E. J. Glover, and C. L. Giles, *Proc. Natl. Acad. Sci.* **99**, 5207 (2002).

[33] M. E. Newman, *Phys. Rev. E* **66**, 016128 (2002).

[34] J. Shao, S. V. Buldyrev, L. A. Braunstein, S. Havlin, and H. E. Stanley, *Phys. Rev. E* **80**, 036105 (2009).

[35] J. Gao et al., *Phys. Rev. E* **88**, 062816 (2013).